IOP Conf. Series: Journal of Physics: Conf. Series **862** (2017) 012003 doi:10.1088/1742-6596/862/1/012003

Expected performance of time-gradient magnetic field SESANS diffractometer at pulsed reactor IBR-2

V Bodnarchuk[1], V Sadilov[1,2], S Manoshin[1], R V Erhan[1,3] and A Ioffe[4]

[1]Joint Institute for Nuclear Research, Frank Laboratory of Neutron Physics, Joliot Curie 6, 141980, Dubna, Moscow region, Russia

[2]Lomonosov Moscow State University, Faculty of Physics, Leninskiye Gory 1, 119991, Moscow, Russia

[3]Horia Hulubei National Institute for R&D in Physics and Nuclear Engineering, Department of Nuclear Physics, Reactorului 30, 077125 Bucharest - Magurele, Romania

[4] Jülich Centre for Neutron Science at Heinz Maier-Leibnitz Centre (JCNS@MLZ), Forschungszentrum Jülich GmbH, Lichtenbergstr. 1, 85747 Garching, Germany

bodnarch@nf.jinr.ru

Abstract. The application of the time-gradient magnetic field neutron spin-echo technique (TGF-NSE) aiming to extend the possibilities of the REFLEX reflectometer at the pulsed reactor IBR-2 (Dubna, Russia) towards a high and medium resolution small-angle scattering is considered. This technique requires the use of a linearly increasing magnetic field in the form of the sequence of saw-teeth pulses. Such a technique is well-suited to the pulsed structure of the neutron beam at the IBR-2 reactor. The wide range of neutron wavelengths employed in the time-of-flight (TOF) operation mode allows for the simultaneous coverage of a wide range of spin-echo lengths (corresponding to a wide Q-range in conventional SANS). Virtual experiments carried out using the VITESS simulation package demonstrate that such a setup at IBR-2 will allow for the coverage of the length scales from 100 Å to 6000 Å in a single instrument setting. The use of the TGF-NSE technique in the TOF mode leads to gaps in the measured SANS curves due to the jumps of magnetic field at the end of saw-teeth pulses. However, crucially, these do not harm the quality of the data. Moreover, the lost data can be retrieved by an additional measurement with a delayed start of the magnetic pulse sequence.

1. Introduction.

Recently, a new time-gradient magnetic field neutron spin echo technique (TGF-NSE) was proposed [1] and tested experimentally [2]. In this technique, the neutron speed is encoded by neutron spin (Larmor) precession in the magnetic field of spin rotators. Such magnetic field is perpendicular to the polarization vector of the neutron beam and increased linearly in time during the time-of-flight of neutrons through the instrument.

By inclining the spin rotators towards the beam axis one can implement the SESANS technique [3] to achieve a high sensitivity to the scattering angle at the sample. This allows the TGF-NSE setup can be used as a small-angle diffractometer or reflectometer [4]. Practically, the application of this TGF-SESANS technique requires the use of linearly increasing magnetic fields in the form of the sequence of saw-teeth pulses. A NSE signal occurs for neutrons passing through the spin rotators during the linear slope of the magnetic field. Consequently, this technique is very well suited to pulsed neutron beams. In this regard, the time-of-flight (TOF) technique a wide range of neutron wavelengths [5] which allows the simultaneous coverage of a wide range of spin-echo lengths (corresponding to a wide Q-range in conventional SANS [3]).

However, the use of the TGF-NSE technique in the TOF mode results in a particular feature that will be discussed in this article on the example of the TGF-SESANS instrument, which is considered for the realization at the pulsed reactor IBR-2 in Dubna, Russia.

2. TGF-SESANS technique at a pulsed beam of the IBR-2 reactor.

The idea of the TGF-NSE technique is to encode the neutron speed by the phase of the neutron spin (Larmor) precession that is acquired during the propagation across the area of magnetic field. Such field is linearly rising in time and perpendicular to the polarization vector of the neutron beam. The phase of the Larmor precession acquired during the neutron propagation across a pair of oppositely directed magnetic field areas (spin rotators) does not depend on the time of the entry of the neutron in the spin rotator, but only on the time required for the propagation in, and between, the two spin rotators forming the arm of the spin-echo spectrometer (figure 1). Similarly to all known NSE techniques [6, 7], the propagation of the neutrons across the second spin-echo arm, which is identical other, however has the opposite direction of magnetic fields, results in the restoration of the polarization of the non-monochromatic neutron beam (the spin-echo focusing).

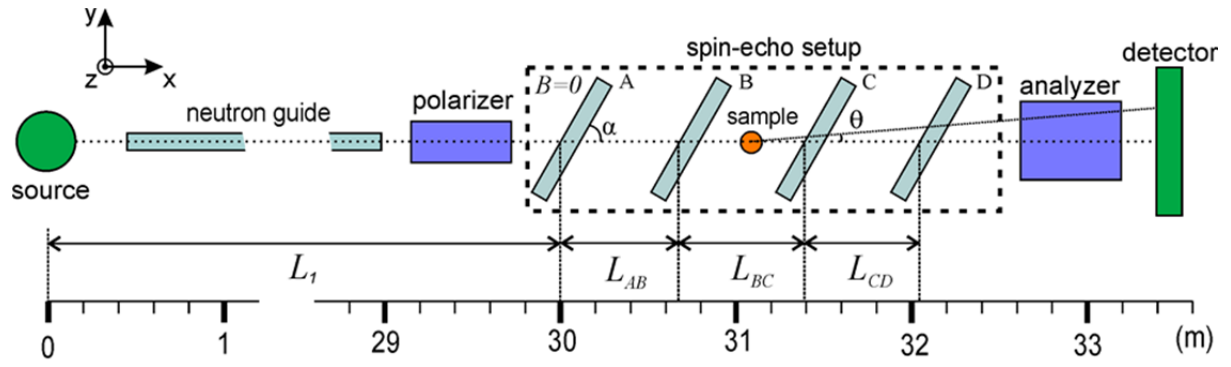

Figure 1. Layout of the SANS instrument using time-gradient magnetic fields (TGF-SESANS). Spin rotators A, B, C and D (of the thickness, a) inclined at an angle, α, to the beam axis are placed in the zero magnetic field volume created by the mu-metal shielding. θ is the angle of scattering on the sample placed between NSE arms. The length scale below shows the position of individual elements with respect to the pulsed neutron source (the reactor core).

The NSE signal occurs for neutrons passing through spin rotators during the linear slope of the magnetic field (figure 2); practically, a sequence of saw-teeth magnetic pulses is used. It should be noted that neutrons which pass the spin rotators during the jump of the magnetic field do not contribute to the NSE signal, as they will acquire a random Larmor precession phase that results in the depolarization of this part of the neutron beam.

The inclination of the spin rotators towards the beam axis of the TGF-NSE instrument yields features of SESANS [4]. In particular, a high sensitivity to the scattering angle θ at the sample placed between two arms. In this case the loss of polarization becomes a measure of the scattering angle θ.

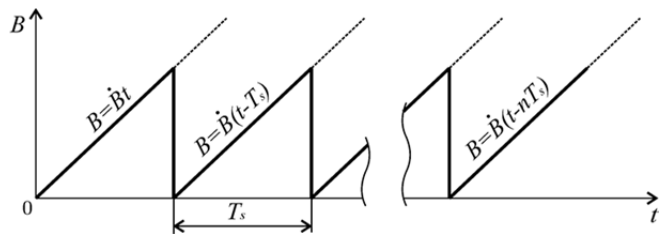

Figure 2. The time structure of the magnetic field in the spin rotators – the sequence of saw-teeth pulse. Only linearly rising parts of the pulses contribute constructively to the NSE signal

In this article we will discuss the use of this technique at neutron beamline 9 of the pulsed reactor IBR-2 in Dubna, where the polarized neutron reflectometer REFLEX [8] is currently operating. For this purpose REFLEX is considered to be additionally equipped with a TGF-SESANS setup formed by two pairs of identical spin rotators, which are tilted at a rather acute angle α (figure 1).

To evaluate the expected performance of TGF-SESANS at IBR-2 we assembled a virtual instrument using the VITESS simulation package [9] extended by dedicated modules to simulate the spin rotators that generate the linearly rising in time magnetic field [10, 11]. The distances between the spin rotators are 71 cm, the thickness of the spin rotators is a = 2 cm, the period of saw-teeth pulses is 5 ms, the amplitude of the pulse is 800 G and angular inclination relative to the instrument axis is 10°. The polarization of the neutron beam is assumed to be 100% over the entire wavelength range.

Evidently, neutrons with different wavelengths will experience either linearly rising magnetic field or field jumps. This magnetic field behavior is illustrated in figure 3, where the several possibilities of neutron propagation time over all four spin rotators are shown.

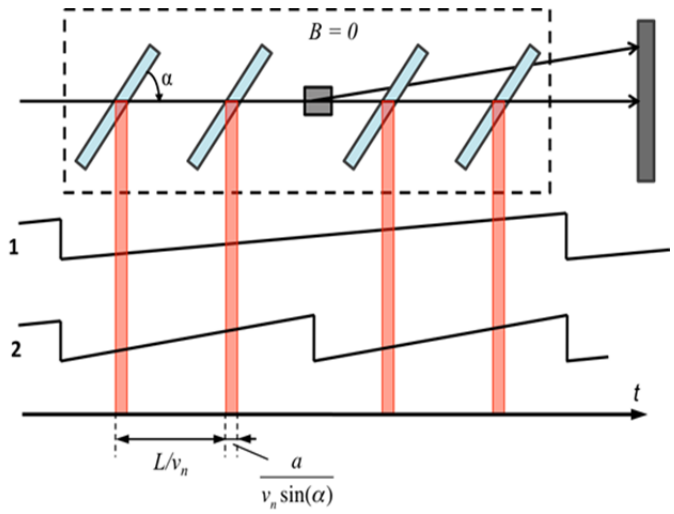

Figure 3. Time diagram illustrating the magnetic field behaviour experienced by neutrons with different wavelengths. For neutrons with shorter wavelengths only one saw-teeth pulse occurs during the neutron propagation time over all four spin rotators (denoted as 1 at the figure). For neutrons with longer wavelength one saw-teeth pulse occurs during the neutron propagation time over two spin rotators (denoted as 2).

The dependence of the polarization, P_z, of the outgoing neutron beam on the wavelength, λ, for the symmetric setup (with equal lengths L_{AB} and L_{CD} of two arms (see figure 1)) is presented in figure 4. Wavelength bands with P_z = 1 correspond to NSE focusing, i.e. to the normal operation of a NSE setup that takes place only for neutrons that experience the linearly rising magnetic fields. Wavelength bands with $P_z < 1$ in figure 4 (left) correspond to neutrons that during their propagation through the setup "experience" a jump of the magnetic field in at least one spin turner: in this case no regular NSE signal is observed.

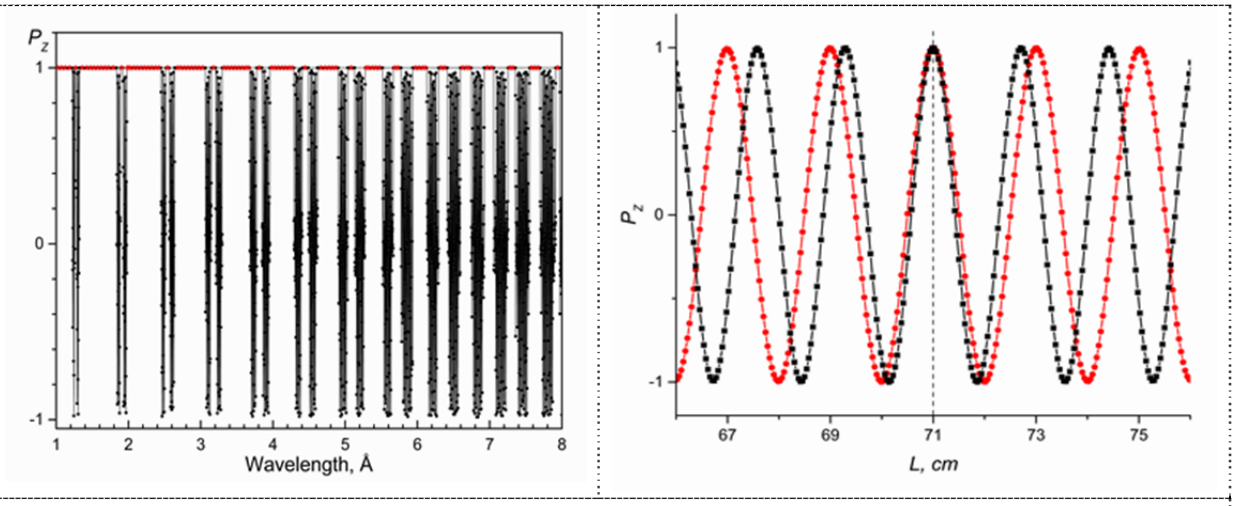

Figure 4. (left) Wavelength dependence of the polarization P_z of the outgoing neutron beam for the symmetric setup without sample. Red dots mark neutron wavelengths used for virtual experiments with samples (see Sect. 3). (right) NSE signals observed for λ = (3.81 ± 0.03) Å (full circles) and λ = (4.02 ± 0.03) Å (full squares) in wide and narrow wavelength bands, respectively.

The position of wavelength bands with P_z = 1 can be explained by means of the L-T diagram presented in figure 5. One can see that for λ = 2.24 Å the neutron propagation across the TGF–NSE setup (spin rotators from A to D) takes place during the rising time of a single *k*-th saw-teeth pulse. However, for λ = 4.43 Å the jump of the magnetic field takes place during the propagation between two spin-echo arms (between rotators B and C), so that neutrons experience two consequent pulses: *k* and (*k*+*1*).

The minimal wavelength of neutrons that experience the begin of *k*-th pulse is

$$\lambda_{min}^{wide} = \frac{h}{m_n}\frac{(k-1)T_s}{L_0} \qquad (1)$$

where m_n is the neutron mass, h is the Planck constant, L_0 is the distance from the source to the spin rotator A and T_s is the duration of the saw-teeth magnetic field pulses. The maximal wavelength of neutrons that experience the end of *k*-th pulse is

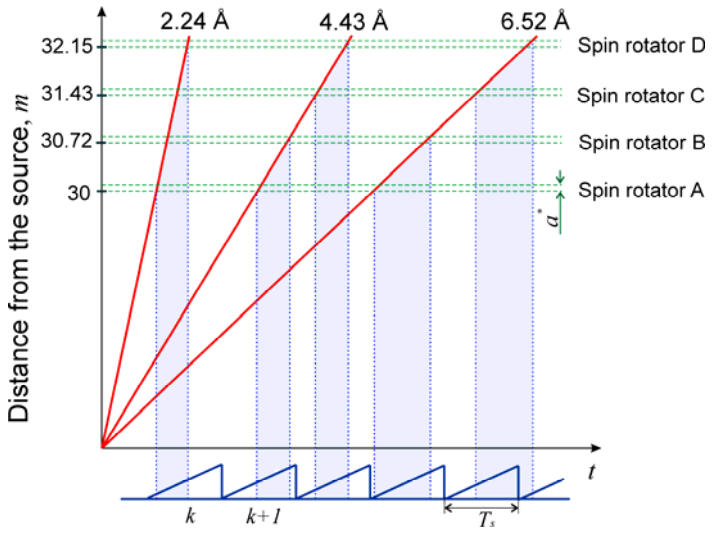

Figure 5. L-T diagram for the TGF-SESANS setup at the IBR-2. (Note that the vertical scale is distorted for the sake of simplicity.) At the bottom of the diagram the sequence of saw-teeth magnetic field pulses synchronized with the 0.24 ms wide reactor pulse (invisible on this scale) are shown. Horizontal lines indicate positions of spin rotators A-D (see figure 1), vertical dashed lines indicate the time when neutrons of different wavelengths cross spin rotators A-D.

$$\lambda_{max}^{wide} = \frac{h}{m_n} \frac{kT_s}{L_0 + L_{AB} + L_{BC} + L_{CD} + a^*} \tag{2}$$

where L_{AB}, L_{BC}, L_{CD} are distances between spin rotators of thickness a (see figure 1), and $a^* = a/\sin(\alpha)$ is the effective thickness of the spin rotators.

The values calculated by Eqs. (1-4) (Table 1) are in excellent agreement with positions of the wide wavelength bands obtained by simulations (figure 4).

Table 1. The values of boundaries of wavelength bands calculated by Eqs. (1-4).

Wide bands		Narrow bands	
λ_{min} (Å)	λ_{max} (Å)	λ_{min} (Å)	λ_{max} (Å)
1.32	1.85	1.26	1.29
1.98	2.46	1.89	1.93
2.64	3.08	2.52	2.57
3.30	3.69	3.15	3.21
3.96	4.31	3.78	3.85
4.61	4.92	4.41	4.49
5.28	5.53	5.03	5.13
5.93	6.15	5.66	5.77
6.59	6.77	6.29	6.42

However, from figure 4 it can be seen that wide wavelength bands are separated by narrow ones. Positions of the latter correspond to the jumps of magnetic field between the NSE arms, so that the pairs of spin rotators A-B and C-D experience linear rising magnetic field, however from two adjacent pulses. The boundaries of these wavelength bands correspond to the end of $(k+1)$-th pulse and are given by

$$\lambda_{min}^{narrow} = \frac{h}{m_n} \frac{(k+1)T_s}{L_0 + L_{AB} + L_{BC}} \tag{3}$$

$$\lambda_{max}^{narrow} = \frac{h}{m_n} \frac{(k+1)T_s}{L_0 + L_{AB} + a^*} \tag{4}$$

These values are again in the excellent agreement with simulations (figure 4 (left)).

3. Virtual experiments.

As a sample for virtual experiments we use homogeneous monodisperse spherical particles with the diameter ranging from 100 Å to 6000 Å. Simulations were carried out only for neutrons within the wavelength bands providing $P_z = 1$ in the empty setup (marked by red dots at figure 4 (left))

The width of the wavelength bands corresponding to $P_z = 1$ is about 0.2 Å, which corresponds to time intervals of about 1.7 ms at the detector. These intervals can be easily selected using a standard multi-channel time analyzer with a channel width of 64 μs; the operation of such a setup is feasible at the IBR-2 reactor.

The neutron beam polarization at the exit of the instrument for a sample scattering at small angles ($\theta << 1$) is given by [12]:

$$P(\lambda) = \frac{\int_{\Omega} F\cos(\Delta\Phi_{TGF})d\Omega}{\int_{\Omega} Fd\Omega}, \quad (5)$$

where the integration is carried out over the solid angle Ω subtended by the analyzer. F is the form-factor of the scattering particle that depends on the scattering angle, θ, neutron wavelength, λ, and the particle radius, R. The phase, $\Delta\Phi_{TGF}$, of the spin precession is given by [4]:

$$\Delta\Phi_{TGF} = 2\gamma B_{max} f_{saw} aL \frac{m_n^2}{h^2} \frac{cot(\alpha)}{sin(\alpha)} \lambda^2 \theta, \quad (6)$$

or, scattering angle, θ, can be expressed by momentum transfer $Q = 2\pi \cdot sin(\theta)/\lambda$ ($\theta << 1$),

$$\Delta\Phi_{TGF}(\theta) = QZ_{TGF} \quad (7)$$

where

$$Z_{TGF} = \frac{1}{2\pi} 2\gamma B_{max} f_{saw} aL \frac{m_n^2}{h^2} \frac{cot(\alpha)}{sin(\alpha)} \lambda^3 \quad (8)$$

is the spin-echo length obtained by the TGF-SESANS setup and is on a physical length scale which correlates to those of the sample being probed. Thus, providing direct information about the particle structure in real space without an intermediate Fourier transform and without the use of reciprocal space.

The results of virtual experiments shown in figure 6 are in a good agreement with the calculations made using Eq. 5. Small gaps ($P_z = 1$) in $P_z(\lambda)$ dependences are noted, however, they do not really harm the result. Moreover, these gaps can be easily closed by an additional measurement made with a slight offset of the saw-teeth sequence with respect to the neutron pulse, i.e. a delayed start of the pulse sequence.

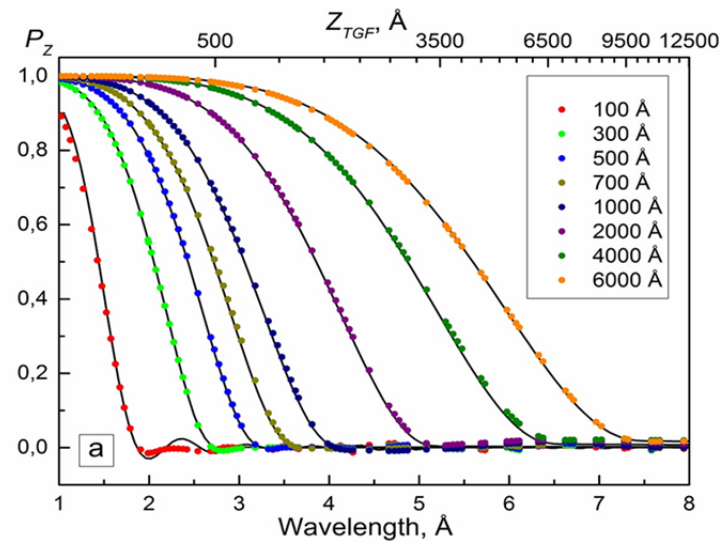

Figure 6. Results of virtual experiments with TGF-SESANS setup. Solid lines are the results of calculations using Eq. (9)

4. Conclusions

The application of the TGF-NSE technique aiming to extend the possibilities of the REFLEX reflectometer at the pulsed reactor IBR-2 (Dubna, Russia) towards a high and medium resolution small-angle scattering is considered. The use of linearly increasing magnetic fields in the form of saw-teeth pulses, is well suited to the pulsed structure of the neutron beam at the IBR-2 reactor.

The wide range of neutron wavelengths employed in the TOF operation mode allows for the simultaneous coverage of a wide range of spin-echo lengths (corresponding to a wide Q-range in conventional SANS, as the latter is proportional to the cube of the neutron wavelength, there is possibilities of SANS studies in a wide length scale). Virtual experiments carried out using VITESS simulation package demonstrate that such a setup at IBR-2 will allow for the coverage of the length scales from 100 Å to 6000 Å in a single instrument setting.

Finally, it should be noted that the use of the TGF-SESANS technique in the TOF mode leads to gaps in the measured SANS curves, caused by the jumps of the magnetic field at the end of the saw-teeth pulses. However, crucially, these do not harm the quality of the data. Moreover, the lost data can be retrieved by an additional measurement with a delayed start of the magnetic pulse sequence.

The financial support from RFBR (grant №14-22-01113-ofi-m) is acknowledged.

References

[1] Ioffe A, Nucl. Instr. and Meth. A **586** (2008) 31–35
[2] Ioffe A, Bodnarchuk V, Bussmann K, Müller R, Georgii R, Nucl. Instr. and Meth. A **586** (2008) 36–40
[3] Rekveldt M Th, Physica B **234–236** (1997) 1135-1137
[4] Ioffe A, Nucl. Instr. and Meth. A **634** (2011) S55-S58
[5] Dalgliesh R M, Langridge S, Plomp J, V.O. de Haan, A.A. van Well, Physica B **406** (2011) 2346–2349
[6] Mezei F, Z. Phyz. **255** (1972) 146
[7] Gahler R, Golub R, J. Phys. C**3-229** (1984) 45
[8] http://flnph.jinr.ru/en/facilities/ibr-2/instruments/reflex
[9] www.helmholtz-berlin.de/vitess
[10] Manoshin S, Ioffe A, Nucl. Instr. and Meth. A **586** (2008) 81–85
[11] Manoshin S.A., Belushkin A.V., Ioffe A., Physics of Particle and Nuclei, V **47**, pp. 667-680 (2016).
[12] Krouglov T, Kraan W H, Plomp J, Rekveldt M Th, Bouwman W G, J. Appl. Cryst. **36** (2003) 816